Controllable dissipation of a qubit coupled to an engineering reservoir

H. Z. Shen,[1,2] Shuang Xu,[1] Su Yi,[3,4,*] and X. X. Yi[1,2,†]

[1]*Center for Quantum Sciences and School of Physics, Northeast Normal University, Changchun 130024, China*
[2]*Center for Advanced Optoelectronic Functional Materials Research, Key Laboratory for UV Light-Emitting Materials and Technology of Ministry of Education, Northeast Normal University, Changchun 130024, China*
[3]*CAS Key Laboratory of Theoretical Physics, Institute of Theoretical Physics, Chinese Academy of Sciences, P.O. Box 2735, Beijing 100190, China*
[4]*School of Physics, CAS Center for Excellence in Topological Quantum Computation, University of Chinese Academy of Sciences, Beijing 100190, China*

(Received 16 August 2018; published 5 December 2018)

The dynamics and non-Markovianity of an atomic impurity qubit (AIQ) immersed in a structured environment is explored where the AIQ is driven by a two-dimensional field and the environment is a quasi-two-dimensional dipolar Bose-Einstein condensate (dBEC). We derive a non-Markovian master equation for the AIQ with initial correlation between the qubit and the dBEC, which contains all the influences of the non-Markovian environment on the atomic impurity qubit. Analyzing the spectrum density for the AIQ-dBEC coupled system and solving the dynamics of the qubit, we find that the atomic impurity qubit can be partially stabilized in its excited state by controlling the x-direction field with the y-direction field fixed. Our analysis reveals that it is the formation of the system-environment bound state that results in such a suppressed dissipation. The present paper is helpful for understanding the effect of the structured and modulated environment and enriches the dynamics of an open system.

DOI: 10.1103/PhysRevA.98.062106

I. INTRODUCTION

All realistic quantum systems interact inevitably with their surrounding environments. Their dynamics can be described by time-dependent collections of completely positive trace-preserving maps [1,2]. The characterization of quantum processes in view of the relationship of these maps at different times leads to the very definition of the Markovian process, which plays an important role in the theory of an open quantum system. Markovian processes successfully describe a plethora of physical processes, particularly in the field of quantum optics, but it fails when it is applied to more complex system-environment couplings where memory effects become important. In recent years a lot of work has been devoted to the study of quantum non-Markovianity. In particular, a notion of memory for quantum processes has been introduced which can be physically interpreted in terms of information flow between the open system and its environments.

The understanding of the implications of non-Markovianity and the reasons for its occurrence are still largely elusive, although there is a growing interest in light of their potential impact on many disciplines from quantum information and nanotechnology to quantum biology [3–6]. An important contribution to this quest came from the formulation of quantitative measures of the degree of non-Markovianity [7–10]. The handiness of such instruments has recently triggered the study of non-Markovianity in quantum many-body systems, such as quantum spin chains [11] or impurity-embedded ultracold atomic systems [12,13] and in excitation-transfer processes in photosynthetic complexes [2].

Many quantum non-Markovian processes described by the dephasing model [14–17] have been observed in quantum optics. High-precision control of Bose-Einstein condensates (BECs) suggests using the atomic BEC as a controllable dephasing reservoir for the qubit [12,18,19] where an impurity atom trapped in a double-well potential acts as the qubit. The information flow between the open system and the reservoir can be observed and well controlled via adjusting the s-wave scattering length.

With the realization of quantum degenerate gases in magnetic atoms [20–24] and heteronuclear molecules [25–27], dipolar BECs (dBECs) have attracted growing attention in recent years. Compared with the BECs where only contact interactions play the key role, dipolar Bose-Einstein condensates have long-ranged and anisotropic dipole-dipole interactions (DDIs), which give rise to a rich array of new physics for ultracold gases [28]. Since non-Markovian dynamics strongly depends on the dephasing factor [9,19], we will carefully examine how the dephasing factor changes with time and its dependence on the dipolar interaction strength. It has been shown that very high densities of states for reservoir modes originate from the roton-type mode softening induced by the DDIs [29–32]. This provides us with a way to nondestructively observe the phenomenon of roton-type mode softening via measuring the dephasing dynamics in Ramsey-type experiment [33]. It is worth stressing that the roton-type modes softening has been observed in the cavity-BEC system [34] and the spin-orbit coupled condensate [35].

*syi@itp.ac.cn
†yixx@nenu.edu.cn

Inspired by cold atomic gases trapped in structured environments [12,13,36,37], we are interested in how and when the dissipation of an atomic impurity qubit (AIQ) coupled to an environment is suppressed. For this purpose, we study the dissipative dynamics of the AIQ driven by a two-dimensional (2D) magnetic field and placed in the structured environment—a quasi-two-dimensional dipolar Bose-Einstein condensate. We derive a non-Markovian master equation with a general entangled initial state, which goes beyond the master equation based on the uncorrelated initial state in the literature [1,38–40]. The expression of spectrum density for the AIQ-dBEC is analytically given. We find that the excited-state population of the atomic impurity qubit would be partially preserved in the steady state by decreasing the x-direction magnetic field at the fixed y-direction magnetic field. This feature can be understood as the formation of the bound state of the whole system (AIQ and dBEC) which results in the suppressed dissipation. This suggests that one can control the dissipation of the AIQ via engineering the bound state of the coupled AIQ-dBEC system.

This paper is organized as follows. In Sec. II, we introduce our model and derive a non-Markovian master equation for the atomic impurity qubit subjected to the dipolar Bose-Einstein condensate environment with an initial correlation between the AIQ and the environment. We analyze the energy spectrum of the whole system (AIQ plus dBEC) and discuss the origin of the suppressed dissipation of the AIQ. In Sec. III, we give an analytical expression of the spectral density and study the non-Markovianity of the system. In Sec. IV, we study the influence of the initial system-environment correlation on the non-Markovian dynamics. Section V is devoted to the discussion of the validity of our model. Finally, we conclude in Sec. VI.

II. THE MODEL AND DYNAMICS

A. The model Hamiltonian

We start by considering a single-atomic impurity qubit immersed in a thermally equilibrated dipolar Bose-Einstein condensate reservoir at temperature T with Rabi frequency ω_z driven by a two-dimensional magnetic field. The Hamiltonian of such a system (system, environment, plus a two-dimensional magnetic field) takes the form

$$\hat{H} = \hat{H}_a + \hat{H}_b + \hat{H}_{ab} + \hat{H}_c, \tag{1}$$

where $\hat{H}_a$ is the Hamiltonian of the impurity atom, $\hat{H}_b$ is the Hamiltonian of the dipolar Bose-Einstein condensate, $\hat{H}_{ab}$ is the interaction Hamiltonian between the impurity and the dipolar Bose-Einstein condensate reservoir, and $\hat{H}_c$ is the interaction Hamiltonian of the impurity atom with the two-dimensional magnetic field.

The impurity atom has two internal states $|+\rangle$ and $|-\rangle$ and is confined in a spin-independent three-dimensional symmetric harmonic trap of the form $V_a(\mathbf{x}) = 1/2 m_a \omega_a^2 \mathbf{x}^2$, where m_a is the mass of the impurity and ω_a is the trap frequency. Under the condition that $\hbar\omega_a \gg k_B T$, we may assume that the spatial wave function of the impurity is the ground state of the harmonic oscillator with potential $V_a(\mathbf{x})$, i.e., $\phi_a(\mathbf{x}) = \pi^{-3/4} L_a^{-3/2} \exp[-\mathbf{x}^2/(2L_a^2)]$, where $L_a = \sqrt{\hbar/(m_a\omega_a)}$. The Hamiltonian for the impurity atom is then,

$$\hat{H}_a = \hbar\Omega_a \hat{\sigma}_z. \tag{2}$$

Here Ω_a is the level splitting between the ground ($|-\rangle$) and the excited ($|+\rangle$) states. For the reservoir atoms, we assume that all dipole moments are polarized along the z axis. The impurity atom-atom interaction is

$$V^{(3D)}(\mathbf{x} - \mathbf{x}_1) = g_b \delta(\mathbf{x} - \mathbf{x}_1) + \frac{3g_d}{4\pi} \frac{1 - 3\cos^2\theta}{|\mathbf{x} - \mathbf{x}_1|^3}, \tag{3}$$

where $g_b = 4\pi\hbar^2 a_B/m_b$ represents the strength of the contact interaction with a_B being the s-wave scattering length, $g_d = \mu_0\mu^2/3$ with μ_0 being the permeability of vacuum, μ being the magnetic dipole moment of the qubit, and θ is the polar angle of $\mathbf{x} - \mathbf{x}_1$. The strength of the dipole-dipole interactions is conveniently measured by the dipolar interaction length $a_D = g_d m_b/(4\pi\hbar^2)$. Moreover, the gas is confined along the z axis by potential $V_b(z) = 1/2 m_b \omega_z^2 z^2$, where ω_z is the trap frequency. For sufficiently large ω_z, the motion of the atoms along the z axis is frozen to the ground state of the oscillator with $V_b(z)$, i.e., $\phi_b(z) = \pi^{-1/4} L_a^{-1/2} \exp[-z^2/(2L_b^2)]$. Following Bogoliubov's method, the Hamiltonian of the reservoir takes

$$\hat{H}_R = \sum_k \hbar\omega_k \hat{a}_k^\dagger \hat{a}_k, \tag{4}$$

where the excitation spectrum [31] is

$$\omega_k = \tfrac{1}{2}\omega_z \sqrt{(L_b k)^4 + P(L_b k)^2 [1 + \chi\alpha(L_b k)]}, \tag{5}$$

where $P = 8\sqrt{2} n L_b a_B$ denotes a dimensionless parameter that characterizes the strength of the contact interaction $L_b = \sqrt{\hbar/(m_b\omega_z)}$, $\chi = g_d/g_b$ being the relative DDI strength, and $\alpha(x) = 2 - 3\sqrt{\pi/2}\, x e^{x^2/2} \mathrm{erfc}(x/\sqrt{2})$ being the Fourier transform of the effective 2D DDI. It is now well established that sufficiently strong DDI would lead to the roton excitation and eventually the instability. Under the given parameters $P = 2$, roton excitation sets in when

$$\chi > \chi^* \approx 4.23. \tag{6}$$

In addition, the condensate becomes unstable for $\chi > \chi^{**} \approx 5.67$. For the interaction Hamiltonian $\hat{H}_{ab}$, we assume that only when the impurity is in the excited-state $|+\rangle$ it undergoes s-wave scattering with atoms in the dipolar Bose-Einstein condensate. Such a collision is characterized by the s-wave scattering length A_{ab}. We note that this scenario can be engineered by means of Feshbach resonances [41] and similar treatments were taken in Refs. [12,42]. Now the interaction Hamiltonian can be written as the following form:

$$\hat{H}_{ab} = \hbar\Omega_b \hat{\sigma}_z + \hat{\sigma}_z \sum_k \hbar g_k (\hat{a}_k + \hat{a}_k^\dagger), \tag{7}$$

where $\Omega_b = 2\sqrt{\pi}\hbar n A_{ab}/[m_{ab}\sqrt{L_a^2 + L_b^2}]$ is the level shift due to the collisions and $m_{ab} = m_a m_b/(m_a + m_b)$ is the reduced mass. And

$$g_k = (n s^{-1/2}) \Omega_b e^{-(L_a k)^2/4} \sqrt{e_k/(\hbar\omega_k)} \tag{8}$$

is the impurity-reservoir coupling parameters with s being the area of the reservoir and $e_k = \hbar^2 k^2/(2m_b)$ being the

free-particle energy. The Hamiltonian for the qubit driven by a two-dimensional magnetic field takes $\hat{H}_m = \hbar B_x \hat{\sigma}_x - \hbar B_z \hat{\sigma}_z$ [43]. For simplicity, we will mainly focus on the resonance case ($\Omega_a + \Omega_b - B_z = 0$), and this requirement can be met by adjusting the magnetic-field B_z in the z direction. After making the unitary transform $\hat{S}=e^{-i(\pi/4)\hat{\sigma}_y}$ to the total Hamiltonian, we arrive at

$$\hat{H} = \hbar B_x \hat{\sigma}_z + \sum_k \hbar\omega_k \hat{a}_k^\dagger \hat{a}_k - \sum_k \hbar g_k \hat{\sigma}_x (\hat{a}_k + \hat{a}_k^\dagger). \quad (9)$$

The interaction Hamiltonian in Eq. (9) contains the counterrotating terms $\hat{\sigma}_- \hat{a}_k$ and $\hat{\sigma}_+ \hat{a}_k^\dagger$. A useful approximation in quantum optics and quantum information communities is the rotating-wave approximation (RWA). With this approximation, Eq. (9) can be written as

$$\hat{H} = \hbar B_x \hat{\sigma}_z + \sum_k \hbar\omega_k \hat{a}_k^\dagger \hat{a}_k - \sum_k \hbar g_k (\hat{\sigma}_+ \hat{a}_k + \hat{a}_k^\dagger \hat{\sigma}_-). \quad (10)$$

Equation (10) is analytically solvable because the total excitation number $\hat{N} = \hat{\sigma}_+\hat{\sigma}_- + \sum_k \hat{a}_k^\dagger \hat{a}_k$ of the whole system is conserved. Due to the tunability of the x-direction magnetic field, we can precisely control the non-Markovian dynamics of the quantum system.

B. The non-Markovian dynamics of the AIQ with the correlated initial state

Due to decoherence phenomena, arbitrary initial states of an infinite bosonic environment are inaccessible in the present experiments. Moreover, according to Ref. [44], the initial system environment correlation cannot be avoided in a realistic situation, and it is therefore reasonable that a more general analysis can give a better understanding of experimental results. We therefore assume the most general formalization of the initial state within the single excitation can be written as

$$|\psi(0)\rangle = \alpha|-,0\rangle + \mathcal{K}(0)|+,0\rangle + \sum_k \mathcal{M}_k(0)|-,1_k\rangle, \quad (11)$$

which is an entangled state of the atomic impurity qubit and dipolar Bose-Einstein condensate [i.e., $\mathcal{M}_k(0) \neq 0$]. Nonetheless, we note that the recent development and progress in the highly controlled experimental techniques allows one to prepare and manipulate systems devised from an increasing number of particles [45]. Our general analysis therefore may also serve as a starting point for studies of reduced dynamics of the qubit coupled to a large but finite bosonic system prepared in a desired quantum state in a single excitation subspace. We note that the initial correlation between system and environment has been extensively investigated both theoretically[46–52] and experimentally [15,53,54]. In particular, Ref. [55] studied an operational approach to open dynamics and quantifying initial correlations.

With this initial state (11), the time-evolved state $|\psi(t)\rangle$ can be written as

$$|\psi(t)\rangle = \alpha|-,0\rangle + \mathcal{K}(t)|+,0\rangle + \sum_k \mathcal{M}_k(t)|-,1_k\rangle, \quad (12)$$

with normalized condition $|\mathcal{K}(t)|^2 + \sum_k |\mathcal{M}_k(t)|^2 = 1$.

By substituting $|\psi(t)\rangle$ into the Schrödinger equation $i\hbar|\dot{\psi}(t)\rangle = \hat{H}|\psi(t)\rangle$, we obtain the equations of motion,

$$\dot{\mathcal{K}} = -iB_x\mathcal{K}(t) - i\sum_k g_k \mathcal{M}_k(t), \quad (13)$$

$$\dot{\mathcal{M}}_k = -i(\omega_k - B_x)\mathcal{M}_k(t) - ig_k\mathcal{K}(t). \quad (14)$$

Solving Eq. (14) for $\mathcal{M}_k(t)$, setting the slowly varying amplitudes transformation $\mathcal{K}(t) \to e^{iB_x t}\mathcal{K}(t)$, $\mathcal{M}_k(t) \to e^{iB_x t}\mathcal{M}_k(t)$, and substituting these into Eq. (13), we obtain the integrodifferential equation,

$$\dot{\mathcal{K}}(t) + 2iB_x\mathcal{K}(t) + \int_0^t \mathcal{K}(\tau)\mathcal{F}(t-\tau)d\tau = \mathcal{S}(t), \quad (15)$$

where the initial value of $\mathcal{K}(t)$ is $\mathcal{K}(0)$. The contribution induced by the initial correlation between system and environment is given by

$$\mathcal{S}(t) = i\sum_k \mathcal{M}_k(0) g_k e^{-i\omega_k t}, \quad (16)$$

and the dissipation-fluctuation kernel,

$$\mathcal{F}(t) = \sum_k |g_k|^2 e^{-i\omega_k t} \equiv \int_0^\infty d\omega J(\omega) e^{-i\omega t}, \quad (17)$$

with spectrum density $J(\omega) = \sum_k |g_k|^2 \delta(\omega - \omega_k)$ being the reservoir spectrum density. In particular, excited-state probability amplitude $\mathcal{K}(t)$ reduces to $\mathcal{K}_0(t)$ when $\mathcal{M}_k(t) = 0$, which is governed by

$$\mathcal{K}_0(t) + 2iB_x\mathcal{K}_0(t) + \int_0^t \mathcal{K}_0(\tau)\mathcal{F}(t-\tau)d\tau = 0, \quad (18)$$

where the initial value is $\mathcal{K}_0(0) = \mathcal{K}(0)$.

In particular, in the continuum limit, $S^{-1}\sum_{\mathbf{k}} \to (2\pi)^{-2}\int d\mathbf{k}$,

$$J(\omega) = \varepsilon\omega_z^3 L_b^4 \int_0^\infty \frac{k^3 e^{-L_a^2 k^2/2}}{\omega(k)} \delta[\omega - \omega(k)]dk, \quad (19)$$

where $\varepsilon = nA_{ab}^2 L_b^2 (m_a + m_b)^2/[m_a^2(L_a^2 + L_b^2)]$ and $\omega(k) \equiv \omega_k$.

The non-Markovian dynamics of the impurity atom system is governed by the exact master equation by tracing over degree of freedom of the reservoir Eq. (12) as follows:

$$\dot{\rho} = -ir(t)[\hat{\sigma}_+\hat{\sigma}_-, \rho] + \gamma(t)[2\hat{\sigma}_-\rho\hat{\sigma}_+ - \hat{\sigma}_+\hat{\sigma}_-\rho - \rho\hat{\sigma}_+\hat{\sigma}_-], \quad (20)$$

where the time coefficients are given by

$$r(t) = -\mathrm{Im}[\dot{\mathcal{K}}(t)/\mathcal{K}(t)], \quad \gamma(t) = -\mathrm{Re}[\dot{\mathcal{K}}(t)/\mathcal{K}(t)]. \quad (21)$$

Detailed derivations of Eq. (22) can be found in Appendix A. Taking the Laplace transformation to Eqs. (15) and (18), respectively, $\mathcal{K}(t)$ can be written as

$$\mathcal{K}(t) = \mathcal{K}(0)\mathcal{K}_0(t) + \int_0^t \mathcal{K}_0(\tau)\mathcal{S}(t-\tau)d\tau, \quad (22)$$

where $\mathcal{K}_0(t)$ is decided by Eq. (18). We show the coherence $r(t)$ and dissipation $\gamma(t)$ contain all the influences of the initial correlations on the system dynamics. In order to see this clearly, we will present an expansion for $r(t)$ and $\gamma(t)$ in orders of the initial population. With this consideration, one can have the coherence and dissipation up to any order in perturbation if required

$$r(t) = r_0(t)\left[1 + \sum_{n=1}^{\infty} \frac{\mathcal{A}(t)^n}{|\mathcal{K}_0(t)|^{2n}}\right] + \frac{\mathcal{B}(t)}{2|\mathcal{K}(t)|^2},$$
$$\gamma(t) = \gamma_0(t)\left[1 + \sum_{n=1}^{\infty} \frac{\mathcal{A}(t)^n}{|\mathcal{K}_0(t)|^{2n}}\right] + \frac{\mathcal{A}(t)}{2|\mathcal{K}(t)|^2}, \tag{23}$$

where $\mathcal{A}(t) = |\mathcal{K}_0(t)|^2 - |\mathcal{K}(t)|^2$, $\mathcal{B}(t) = 2\,\mathrm{Im}(\dot{\mathcal{K}}_0\mathcal{K}_0^* - \dot{\mathcal{K}}\mathcal{K}^*)$, and

$$r_0(t) = -\mathrm{Im}[\dot{\mathcal{K}}_0(t)/\mathcal{K}_0(t)],$$
$$\gamma_0(t) = -\mathrm{Re}[\dot{\mathcal{K}}_0(t)/\mathcal{K}_0(t)], \tag{24}$$

which corresponds to the coherence and dissipation in the uncorrelated initial state $[\mathcal{M}_k(0) = 0]$ with the master equation $\dot{\rho}_0 = -ir_0(t)[\hat{\sigma}_+\hat{\sigma}_-, \rho_0] + \gamma_0(t)\,[2\hat{\sigma}_-\rho_0\hat{\sigma}_+ - \hat{\sigma}_+\hat{\sigma}_-\rho_0 - \rho_0\hat{\sigma}_+\hat{\sigma}_-]$, where $\rho_0 = |\mathcal{K}_0(t)|^2|+\rangle\langle+| + [1 - |\mathcal{K}_0(t)|^2]|-\rangle\langle-|$, which is consistent with the case of the uncorrelated initial state [1,38–40]. With Eqs. (20) and (22), we can study the exact time-dependent non-Markovian dynamics for the AIQ when the system and environment initially are prepared in a correlated state (11). From the above results, we find that the first term in Eq. (24) represents the zero-order approximation, which corresponds to the uncorrelated initial state $[\mathcal{M}_k(0) = 0]$. The other terms of Eq. (24) except the first term denote the influence of the high-order contributions for the initial correlations ($n \geqslant 1$) to the system dynamics.

As a concrete example, we consider a single ^{87}Rb atom immersed in a dBEC of ^{164}Dy atoms [22,23]. The dipolar interaction length a_D for ^{164}Dy atoms is around 7 nm, and the s-wave scattering length between Dy atoms is $a_B = 5.3$ nm [22,23], which leads to the dipolar-contact interaction ratio $\chi \sim 1.32$. In general, we will treat χ as a control parameter which can, in principle, be realized by tuning a_B through the Feshbach resonance. The parameters P and ε can be estimated as follows. For a typical trap frequency $\omega_z = 2\pi \times 10^3$ Hz, the corresponding harmonic-oscillator width is $L_b \sim 2.5 \times 10^{-5}$ cm. Assuming that the peak density of the condensate is 10^{14} cm^{-3}, the area density is then $n = 4.4 \times 10^9$ cm^{-2}, which results in the typical value of $P \sim 1.5$. To fix ε, we assume that the s-wave scattering length between ^{87}Rb and ^{164}Dy atoms is $A_{ab} \sim 5$ nm and the width of the impurity trap L_a equals the dBEC trap length L_b and we therefore have $\varepsilon \sim 4.6 \times 10^{-3}$. Without loss of generality, we will take $P = 2$, $\varepsilon = 0.0046$ in the simulation.

In Fig. 1, we plot $|\mathcal{K}_0(t)|$ in Eq. (18) for different B_x's. We can see that $|\mathcal{K}_0(t)|$ decays fast after transient oscillations for strong B_x. We will refer to the dynamics in this regime as the complete decoherence [see Figs. 1(b), 1(d) and 1(f)]. With the decrease in the magnetic field, the decay is suppressed, which is dramatically different from that a weaker driving strength always induces a more severe decoherence. When

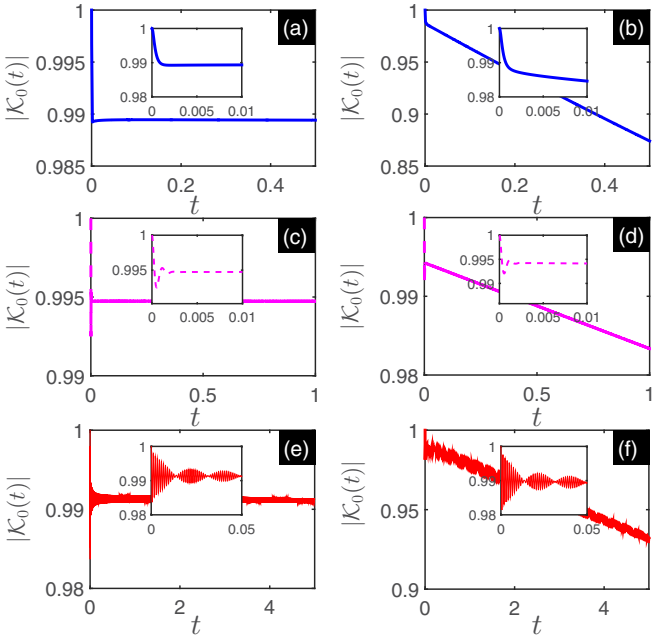

FIG. 1. The figure shows the time evolution of the exact solution $|\mathcal{K}_0(t)|$. Here we have taken the parameters $\chi = 0$ for (a) and (b), $\chi = 2$ for (c) and (d), and $\chi = 4.6$ for (e) and (f). $B_x = 10$ Hz for (a), (c), and (e) and $B_x = 100$ Hz for (b), (d), and (f).

$B_x = 10$ Hz, the coherence does not decay to zero, and a finite quantum coherence is preserved in the steady state. With the increase in the relative DDI strength χ, the oscillation is totally stabilized, and the decoherence is inhibited. We call the dynamics in this regime $B_x \leqslant B_x^{cl}/2$ (see the next subsection) as decoherence suppression.

This observation indicates that the system encounters a threshold induced by the non-Markovian effect. Although this result confirms that the memory function connects directly with the non-Markovianity, the existence of the threshold point B_x inspires us to further pursue the hidden physical reason for the system.

C. Energy spectrum of the AIQ-dBEC system

In this section, we will show that the decoherence suppression for the atomic impurity qubit system is due to the bound state of the whole system (atomic impurity qubit plus environment) [56–60]. Possible observations of the prediction can be observed within current technologies [61–64]. To proceed, we perform a Laplace transform to Eq. (18) and obtain $\bar{\mathcal{K}}_0(s) = [s + iB_x + \bar{\mathcal{F}}(s)]^{-1}$ with $\bar{\mathcal{F}}(s) = \int_0^\infty \frac{J(\omega)}{s+i\omega-iB_x} d\omega$ [In order to maintain consistency with the eigenequation below, here we have used $\mathcal{K}_0(t)$ without rotation to B_x, i.e., $\mathcal{K}_0(t)$ satisfies $\mathcal{K}_0(t) + iB_x\mathcal{K}_0(t) + \int_0^t \mathcal{K}_0(\tau)\mathcal{F}(t-\tau)d\tau = 0$ with $\mathcal{F}(t) = \int_0^\infty d\omega J(\omega)e^{-i(\omega-B_x)t}$, please see below Eq. (14)]. According to the Cauchy residue theorem, the inverse Laplace transform can be performed by finding all the poles of $\bar{\mathcal{K}}_0(s)$. We now consider a special case if there is a pole on the imaginary axis, i.e., purely imaginary axis $s = -iE_{bs}$ (E_{bs} is a real number)in which poles equation,

$$s + iB_x + \bar{\mathcal{F}}(s) = 0 \tag{25}$$

leads to the identity,

$$B_x + \int_0^\infty \frac{J(\omega)}{B_x - \omega + E_{bs}} d\omega = E_{bs}, \tag{26}$$

where $J(\omega)$ is given by Eq. (19). Note that the roots of Eq. (26) are just the eigenenergies in the single-excitation subspace of the whole system consisting of the AIQ and its environment. To see this, we expand the eigenstates as $|\Phi\rangle = \mathcal{Z}|+, \{0_k\}\rangle + \sum_k u_k|-, 1_k\rangle$. Then from the eigenequation,

$$\hat{H}|\Phi\rangle = E|\Phi\rangle, \tag{27}$$

with Hamiltonian given by Eq. (10), we obtain

$$\sum_k g_k u_k = -(E - B_x)\mathcal{Z}, \tag{28}$$

$$g_k \mathcal{Z} = -u_k(B_x + E - \omega_k). \tag{29}$$

For the bound-state energy $E < -B_x$, solving Eq. (29) gives $u_k = -g_k\mathcal{Z}/(B_x + E - \omega_k)$. Equation (26) can be obtained by substituting the result u_k into Eq. (28). In this regime with $|\mathcal{Z}|^2 + \sum_k |u_k|^2 = 1$, we obtain

$$\mathcal{Z}(E_{bs}) = \left[1 + \sum_k \frac{g_k^2}{(B_x - \omega_k + E_{bs})^2}\right]^{-1/2}. \tag{30}$$

It is interesting to see that the roots of Eq. (26) multiplied by $\hbar$ are just the eigenenergies in the single-excitation subspace, see Eq. (10). It is understandable from the fact that the decoherence of the AIQ induced by the vacuum environment is governed by the single-excitation process of the whole system. For the sake of discussion about the critical equation of the bound states below, we define the left side of Eq. (26) as

$$X(E_{bs}) \equiv B_x + \int_0^\infty \frac{J(\omega)}{B_x - \omega + E_{bs}} d\omega. \tag{31}$$

Since $X(E_{bs})$ is a monotonically decreasing function when $E_{bs} < -B_x$, Eq. (26) has one discrete root if $X(-B_x) < -B_x$. It has an infinite number of roots in the region $E_{bs} > -B_x$, which form a continuous energy band. We name this discrete eigenstate with eigenenergy $E_{bs} < -B_x$ the bound state. Its formation would have profound consequences on the decoherence dynamics. Equation (26) has an isolated root in the band gap whenever

$$2B_x \leqslant \int_0^\infty \frac{J(\omega)}{\omega} d\omega \equiv B_x^{cl}. \tag{32}$$

To see this, we perform the inverse Laplace transform to $\bar{\mathcal{K}}_0(s)$, and obtain

$$\mathcal{K}_0(t) = \mathcal{Z}^2(E_{bs})e^{-iE_{bs}t} + \int_{i\varsigma+0}^{i\varsigma+\infty} \frac{d\omega}{2\pi} \bar{\mathcal{K}}_0(-i\omega)e^{-i\omega t}, \tag{33}$$

where $\mathcal{Z}(E_{bs})$ is given by Eq. (30) and the second term contains contributions from the continuous energy band. Oscillating with time in continuously changing frequencies, the second term in Eq. (33) decays and tends to zero due to out-of-phase interference. Therefore, if the bound state is absent, then $\lim_{t\to\infty}\mathcal{K}_0(t) = 0$ characterizes a complete decoherence, whereas if the bound state is formed, then $\lim_{t\to\infty}\mathcal{K}_0(t) = \mathcal{Z}^2(E_{bs})e^{-iE_{bs}t}$ implies dissipation suppression.

To make this result clear, we recall that, according to the Schrödinger equation, $i\hbar(\partial/\partial t)|\psi(t)\rangle = \hat{H}|\psi(t)\rangle$ with $\hat{H}$ given by Eq. (10). The time evolution of the whole state satisfies $|\psi(t)\rangle = e^{-i\hat{H}t/\hbar}|+, 0\rangle$. Inserting completeness relations $|\Phi_{bs}\rangle\langle\Phi_{bs}| + \int_{-B_x}^\infty |\Phi_c(E_c)\rangle\langle\Phi_c(E_c)|dE_c = I$ into it, we obtain

$$|\psi(t)\rangle = \mathcal{Z}(E_{bs})e^{-iE_{bs}t}|\Phi_{bs}\rangle + |\psi_c(t)\rangle, \tag{34}$$

where $|\psi_{bs}(t)\rangle$ denotes the bound state with energy E_{bs} given by Eq. (26). $|\psi_c(t)\rangle$ is a superposition of the continuous-spectrum eigenfunctions of the Hamiltonian,

$$|\psi_c(t)\rangle = \int_{-B_x}^\infty e^{-iE_c t}\mathcal{Z}_c^*(E_c)|\Phi_c(E_c)\rangle dE_c, \tag{35}$$

with the continuous-spectrum eigenfunctions,

$$|\Phi_c(E_c)\rangle = \mathcal{Z}_c(E_c)|+, \{0_k\}\rangle + \int_0^\infty u_{c,k}(E_c)|-, 1_k\rangle dk, \tag{36}$$

where E_c denotes the continuous-spectrum eigenenergy in the regime of $E_c > -B_x$, which is obtained by the diagonalization of

$$\hat{H}_{se} = \begin{pmatrix} B_x & -g_1 & \cdots & -g_N \\ -g_1 & \omega_1 - B_x & 0 & 0 \\ \cdots & 0 & \cdots & 0 \\ -g_N & 0 & 0 & \omega_N - B_x \end{pmatrix}, \tag{37}$$

where N denotes total mode numbers of the structured environment and $\mathcal{Z}_c(E_c)$ and $u_{c,k}(E_c)$ are solved in the regime of $E_c > -B_x$ by Eqs. (28) and (29), respectively. The probability amplitude on the upper state from Eq. (34) can be written as

$$\mathcal{Z}^2(E_{bs})e^{-iE_{bs}t} + \int_{-B_x}^\infty e^{-iE_c t}|\mathcal{Z}_c^2(E_c)|dE_c. \tag{38}$$

We show that the second term of Eq. (38) corresponds to the second term of Eq. (33), which tends to zero in the long-time limit $t \to \infty$ according to the Lebesgue-Riemann lemma [65]. This leads to the probability amplitude on the upper state to approach $\mathcal{Z}^2(E_{bs})e^{-iE_{bs}t}$. Note that this feature has been illustrated in the literature [56,66] to describe the incomplete decay of an atom in photonic band-gap media.

According to critical equation (32), we can calculate $B_x^{cl} = 33.77$ Hz for $\chi = 0$, $B_x^{cl} = 30.57$ Hz for $\chi = 2$, and $B_x^{cl} = 50.74$ Hz for $\chi = 4.6$. The energy spectrum E and the decay rate $\gamma(t)$ are shown in Fig. 2. We can see that $\gamma(t)$ tends to a positive constant in the absence of the bound state when $B_x > B_x^{cl}/2$. The complete positivity of $\gamma(t)$ causes $|\mathcal{K}_0(t)|$ to decay to zero monotonically. Here the dipolar Bose-Einstein condensate reservoir has no backaction on the system. When the bound state is formed with $B_x \leqslant B_x^{cl}/2$, the competition between the environmental backaction and the dissipation on the impurity atom causes $\gamma(t)$ to transiently take negative values and asymptotically approaches zero [see Figs. 2(c) and 2(e)]. Consequently, after some short-time oscillations, $|\mathcal{K}_0(t)|$ tends to a finite value matching well with the result $\lim_{t\to\infty}\mathcal{K}_0(t) = \mathcal{Z}^2(E_{bs})e^{-iE_{bs}t}$.

The phase diagram derived from Eq. (32) is quite rich, see Fig. 3. The dashed-pink line shows the first critical equation

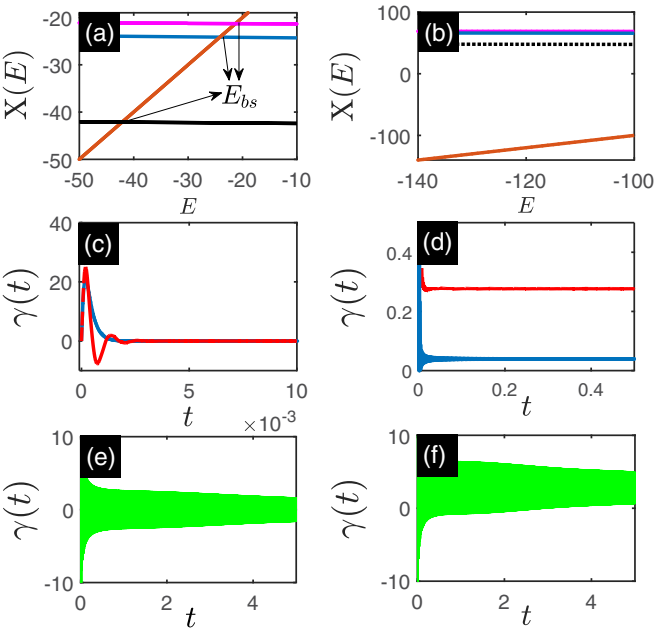

FIG. 2. (a) and (b) Diagrammatic solutions of Eq. (26) with different parameters $\chi = 0$, $\chi = 2$, and $\chi = 4.6$ correspond to dashed-blue, solid-pink, and dotted-black lines, respectively. $B_x = 10$ Hz for (a), $B_x = 100$ Hz for (b). (c)–(f) The time evolution of the dissipation coefficient. Here we have taken the parameters $\chi = 0$ for the blue lines in (c) and (d), $\chi = 2$ for the dashed-red lines in (c) and (d). $\chi = 4.6$ for (e) and (f). $B_x = 10$ Hz for (c) and (e). $B_x = 100$ Hz for (d) and (f).

in Eq. (32). The existence of the quantum phase transition (QPT) in the model can be clearly found. The ground-state energy and its derivative are plotted in Figs. 3(b) and Fig. 3(c), respectively. At zero temperature, the nonanalyticity of the ground-state energy is directly connected to the QPT. The first-order QPT is characterized by the discontinuity in the first derivative of the ground-state energy with respect to χ. It is easy to find that the first derivative is discontinuous at the critical point (32), which means that it is a first-order QPT.

III. ANALYTICAL EXPRESSION OF THE SPECTRAL DENSITY AND NON-MARKOVIANITY

A. Analytical solution of the spectral density

The physics behind the dynamics of the atomic impurity qubit can be found by examining the system-environment spectrum density. To this end, we plot the corresponding spectral density $J(\omega)$ in Fig. 4. Clearly, for $\chi = 0$, $J(\omega)$ is a function peaked at $\omega = 0.9\omega_z$, see the blue-thin line of Fig. 4(a). The peak of $J(\omega)$ then moves to ω_z when the DDI is turned on, see the red-thick line of Fig. 4(a). In particular, $J(\omega)$ becomes a sharply peaked function as χ approaches χ^* [see Fig. 4(b)]. Intuitively, a peak at ω_q on $J(\omega)$ indicates that the spectral density is particularly high at ω_q, which picks up the frequency ω_q for the non-Markovian dissipative rate $\gamma(t)$ through Eq. (22) and results in oscillating in $\mathcal{K}_0(t)$. To see this more clearly, we approximate $J(\omega)$ as a δ function, i.e., $J(\omega) \approx \sum_q C_q \delta(\omega - \omega_q)$ with an amplitude

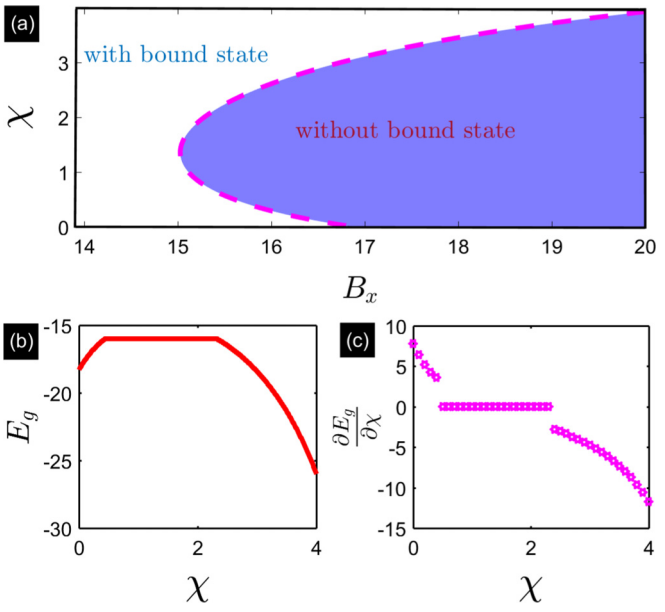

FIG. 3. (a) Phase diagram of the atomic impurity qubit in the space spanned by the DDI strength and the field B_x. The dashed-pink line is given by the critical equation (32): $2B_x = \int_0^\infty \frac{J(\omega)}{\omega} d\omega$. (b) Ground-state energy E_g given by Eq. (26) with $B_x = 16$ Hz and (c) its first derivative $\frac{\partial E_g}{\partial \chi}$ with respect to χ as a function of the relative DDI strength with $B_x = 16$ Hz.

C_q (q indicates the number of the peaks) in which we obtain immediately the correlation function $\mathcal{F}(t) \approx \sum_q C_q e^{-i\omega_q t}$ in Eq. (17), an undamped oscillating function of t. In the case of $\chi = 4.6$ as shown in Fig. 4(b), we find that there exists a so-called "beat frequency" phenomenon for coupling between

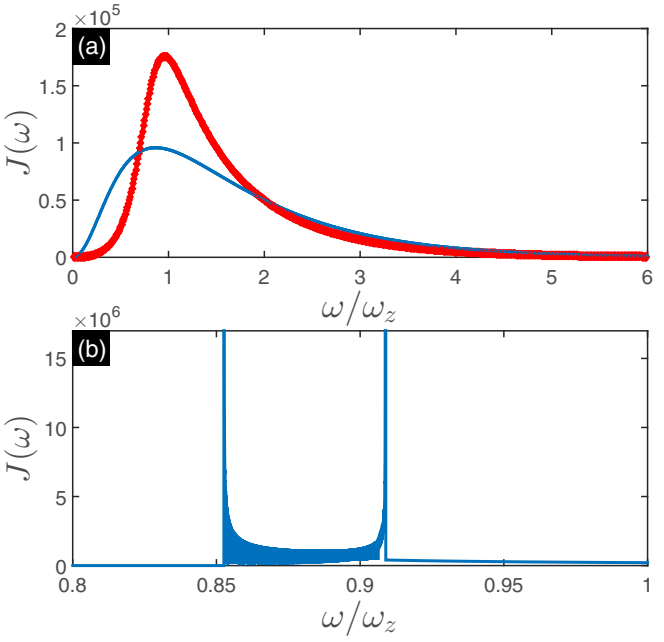

FIG. 4. The spectrum density function given by Eq. (39). The blue-thin and red-thick lines correspond to $\chi = 0$ and $\chi = 2$, respectively, in (a). In (b), χ takes 4.6.

system and environment, which originates from the two peaks in the dependence of $J(\omega)$ on ω. In the following, we will give approximately an analytical expression for $J(\omega)$.

We assume that $k_j(\omega)$ is the root of equation $\omega = \omega_k$ with ω_k given by Eq. (5), so the spectral density of the AIQ-dBEC system in Eq. (19) reduces to

$$J(\omega) = \varepsilon\hbar^2\omega_z^3 L_b^4 \sum_j \frac{\lambda[k_j(\omega)]}{\omega}\left|\frac{d\omega_k}{dk}\right|^{-1}_{k=k_j(\omega)}, \tag{39}$$

where $\lambda(k) = k^3 e^{-L_a^2k^2/2}$. When $\chi > \chi^*$, the exciton spectrum has a local maximum as k_M and a local minimum at k_m, the corresponding exciton energies are $\hbar\omega_M = \hbar\omega_{k_M}$ and $\hbar\omega_m = \hbar\omega_{k_m}$, respectively. Based on Eq. (39), $J(\omega)$ diverges at ω_M and ω_m. To accurately take into account the contributions from these singularities to $J(\omega)$, let us focus on ω_k in the vicinities of k_M where the excitation energy can be approximated as $\omega_k \simeq \omega_M + \omega_k''(k_M)(k-k_M)^2/2$. Using Eq. (39), it can be then shown that, in the vicinity of ω_M, we have $J(\omega) = Z_M(\omega_M-\omega)^{-1/2}$ for $\omega < \omega_M$, where $Z_M = \sqrt{2\hbar^{1.5}}\varepsilon\omega_z^3 L_b^4\lambda(k_M)|\omega_k''(k_M)|^{-1/2}/\omega_M$. Similarly, in the vicinity of the local minimum, we have $J(\omega) = Z_m(\omega_m-\omega)^{-1/2}$ for $\omega > \omega_m$, where $Z_M = \sqrt{2\hbar^{1.5}}\varepsilon\omega_z^3 L_b^4\lambda(k_m)|\omega_k''(k_m)|^{-1/2}/\omega_m$.

Based on the above discussion, we may assume that these two singularities result in the largest contribution to system-environment spectrum density $J(\omega)$. We then define

$$\tilde{J}(\omega) = Z_M\frac{\theta(\omega_M-\omega)}{(\omega_M-\omega)} + Z_m\frac{\theta(\omega-\omega_m)}{(\omega-\omega_m)}, \tag{40}$$

as the approximate $J(\omega)$, where $\theta(t)$ is the unit step function that $\theta(t)$ equals one when t is greater than or equal to zero, otherwise $\theta(t)$ is zero.

With this approximation, the expression of $\mathcal{K}_0(t)$ for the general spectrum density can be calculated using the analytical expressions by the Laplace transformation [67],

$$\mathcal{K}_0(t) = \mathcal{Z}^2(E_{bs})e^{-iE_{bs}t} + \frac{1}{\pi}\int_{-\infty}^{\infty}d\omega \times \frac{\mathcal{I}(\omega)e^{-i\omega t}}{[\omega-2B_x-\mathcal{R}(\omega)]^2+\mathcal{I}^2(\omega)}, \tag{41}$$

where E_{bs} is given by Eq. (26) and $\mathcal{R}(\omega) = \mathrm{P}\int_{-\infty}^{\infty}\frac{J(\omega')d\omega'}{\omega-\omega'}$ and $\mathcal{I}(\omega) = \pi J(\omega)$. Due to the vanishing spectral density for $E_{bs} < 0$, a localized mode at $\mathrm{X}(E_{bs}) = 0$ occurs for $E_{bs} < 0$. The localized mode that leads to the dissipationless process is given by Eq. (33). Equation (41) shows that the environment modifies the system spectrum as a combination of localized modes (dissipationless process) plus a continuum spectrum part (nonexponential decays). Remarkably, the result obtained from these simple examples gives indeed the underlying structure of memory functions in arbitrary complicated systems. This indicates that alternatively, non-Markovian dynamics can be fully characterized by the environmental-modified spectrum of the system.

Figure 5 shows the comparison of $|\mathcal{K}_0(t)|$ and $|\tilde{\mathcal{K}}_0(t)|$ for $\chi = 5.6$ and $\chi = 4.7$, respectively. The parameters $Z_{m,M}$ and $\omega_{m,M}$ used in $|\tilde{\mathcal{K}}_0(t)|$ are all obtained with the given χ with the excitation spectrum (5). As the DDI strength decreases, for example, $\chi = 4.7$, ω_M (ω_m) decreases (increases) such that Z_M becomes much larger than Z_m. We find from Fig. 5 that the results given by the approximate analytical solution Eq. (40) are in good agreement with those obtained by the numerical simulation based on Eq. (39).

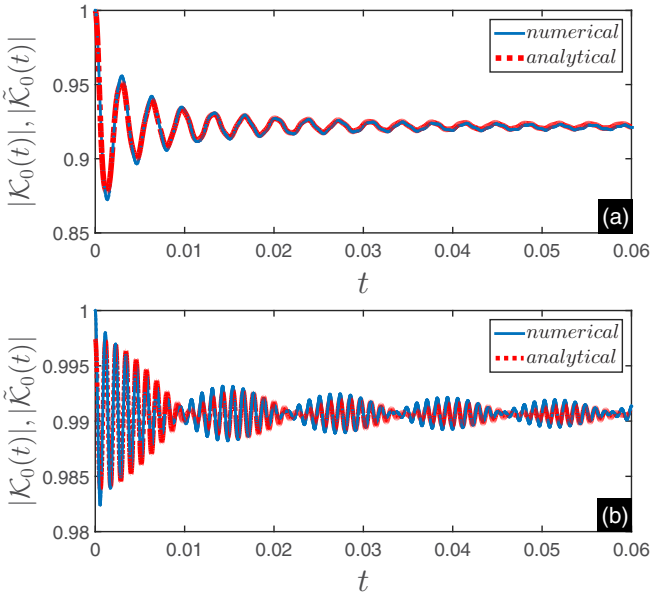

FIG. 5. $|\mathcal{K}_0(t)|$ and $|\tilde{\mathcal{K}}_0(t)|$ versus time t. The dotted and solid lines correspond to the analytical expression $|\tilde{\mathcal{K}}_0(t)|$ given by Eq. (41) based on Eq. (40), whereas $|\mathcal{K}_0(t)|$ is for the fully numerical simulation by solving Eq. (39). $|\mathcal{K}_0(t)|$ and $|\tilde{\mathcal{K}}_0(t)|$ are plotted for (a) $\chi = 5.6$ and (b) $\chi = 4.7$. Parameters chosen in (a) are $B_x = 10$ Hz, $Z_M/\omega_z^{1/2} = 49.49$, $\omega_M/\omega_z = 0.933$, and $Z_m/\omega_z^{1/2} = 12.30$, $\omega_m/\omega_z = 0.25$; $Z_M/\omega_z^{1/2} = 38.83$, $\omega_M/\omega_z = 0.91$, and $Z_m/\omega_z^{1/2} = 21.38$, $\omega_m/\omega_z = 0.83$ for (b).

B. Non-Markovianity for the atomic impurity qubit in dBEC

To study the non-Markovianity of the quantum process, we should take away the contribution from the initial states. This consideration suggests taking an uncorrelated state as the initial one. The following measure of non-Markovianity will be used in the discussion:

$$\mathcal{N} = \max_{\rho_{1,2}(0)}\int_{\sigma(t)>0} dt\,\sigma(t), \tag{42}$$

where $\sigma(t) = \dot{\mathcal{D}}[\rho_1(t), \rho_2(t)]$ is the change rate of the trace distance $\mathcal{D}[\rho_1(t), \rho_2(t)] = \frac{1}{2}\mathrm{Tr}|\rho_1(t) - \rho_2(t)|$ between states $\rho_1(t)$ and $\rho_2(t)$ with their respective initial states $\rho_1(0)$ and $\rho_2(0)$ [9]. In the Markovian limit, the environment acts, such as a "sink" that all the energy flows irreversibly from the system to the environment. The states become more and more indistinguishable with time, which means $\sigma(t) < 0$ always holds, and thus $\mathcal{N} = 0$. In the non-Markovian dynamics, the dynamical interplay between the system and the environment would transiently cause the energy backflow from the environment to the system. This would lead to the increase in the distance.

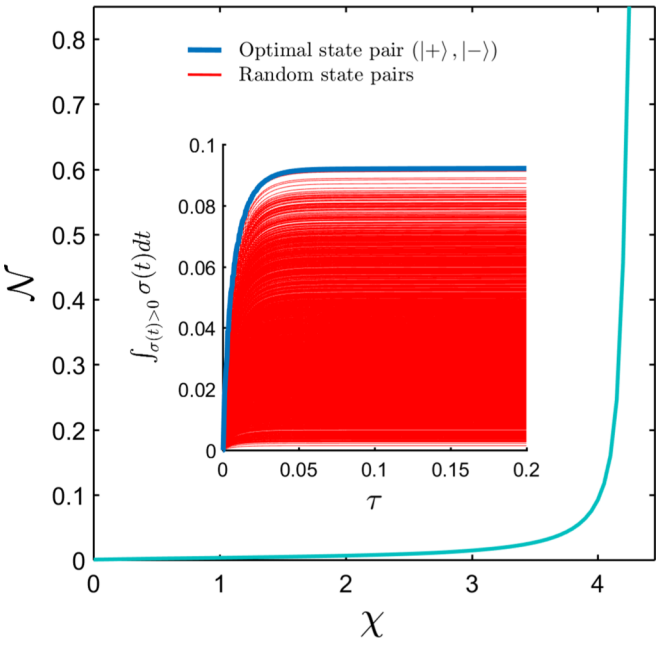

FIG. 6. Non-Markovianity $\mathcal{N}$ as a function of the relative DDI strength χ with $B_x = 10$ Hz. The inset shows the integrals $\int_{\sigma(t)>0}\sigma(t)dt$ in the definition of non-Markovianity [Eq. (42)] versus the driving time σ with $\chi = 4$. The blue and red lines represent the integrals with initial states $(|+\rangle, |-\rangle)$ and the other 2000 randomly chosen pairs, respectively.

There exists no general analytical expression for the optimal initial states $\rho_1(0)$ and $\rho_2(0)$ [68]. But for a given pair of $\rho_1(0)$ and $\rho_2(0)$, the distance is given by

$$\mathcal{D}(\rho_1, \rho_2) = |\mathcal{K}_0|\sqrt{A^2|\mathcal{K}_0|^2 + B^2}, \tag{43}$$

where $A = \rho_1(t=0)^{11} - \rho_2(t=0)^{11}$ and $B = \rho_1(t=0)^{10} - \rho_2(t=0)^{10}$ are defined by the elements of the initial density matrix and Eq. (42) has been used.

In Fig. 6, the integral $\int_{\sigma(t)>0}\sigma(t)dt$ in the definition of $\mathcal{N}$ with 2000 randomly chosen initial states $[\rho_1(0), \rho_2(0)]$ [denoted by thin-red curves] is plotted (with $\chi = 2$). Clearly all these pairs yield smaller values than that of the state pair $(|+\rangle, |-\rangle)$ (denoted by the bold-blue curve). This suggests that $|+\rangle$ and $|-\rangle$ are the optimal pair, which maximizes the change rate in Eq. (42). Thus the trace distance of the evolved states can be written as $\mathcal{D}(t) = |\mathcal{K}_0(t)|^2$. Based on this observation, we write the non-Markovianity as

$$\mathcal{N} = \frac{1}{2}\left[|\mathcal{K}_0(\tau)|^2 - 1 + \int_0^\tau |\partial_t|\mathcal{K}_0(t)|^2|dt\right], \tag{44}$$

where τ denotes the time when the system reaches the steady state. We show in this case that the non-Markovianity measure (42) given by the trace distance is equivalent to measures based on divisibility with Ref. [8]. For a slightly larger χ, we find it is very difficult to obtain a converged $\mathcal{N}$. As expected, $\mathcal{N}$ increases very quickly when χ approaches the divergent point χ^*.

So far, we have studied the non-Markovian dynamics for the atomic impurity qubit immersed in the dipolar Bose-Einstein condensate. In the next section, we will discuss the influence of initial system-environment correlation on the system dynamics.

IV. INFLUENCE OF THE INITIAL CORRELATION ON NON-MARKOVIAN DYNAMICS

In the previous section, we have found a threshold χ^* in the influence of the dipolar Bose-Einstein condensate on the dynamics of the atomic impurity qubit; this is a prediction of the non-Markovian effect in open quantum systems. In this section, we will study the effect of initial system-environment correlation on the system. The steady state of the system in Eq. (22) including the initial correlation between the AIQ and the dBEC reads (11)

$$\mathcal{K}(t)|_{t\to\infty} = \frac{e^{-iE_{bs}t/\hbar}}{\{\tilde{\mathcal{K}}[-iE_{bs}/\hbar]^{-1}\}'}\left[\mathcal{K}(0) - \frac{\sum_k \mathcal{M}_k(0)g_k}{E_{bs}/\hbar - 2B_x}\right], \tag{45}$$

where $\{\cdots\}'$ denotes the first derivative of $\{\cdots\}$ with respect to E_{bs}. In the following, two examples will be used to exemplify the initial correlation effects.

This first is the *sinusoidal wave case*. Consider an initial probability amplitude taking the sinusoidal form

$$\mathcal{M}_k(0) = \begin{cases} i\eta\ \sin[a(k-k_0)/\Delta_0]/\sqrt{\Delta_0 S}, & 0 \leqslant k \leqslant T_0, \\ 0, & k > T_0, \end{cases} \tag{46}$$

where k_0 is the wave vector corresponding to the central frequency of the dNEC reservoir, η is the distribution intensity in the non-Markovian environment, Δ_0 is the width, and T_0 is the period of the sinusoidal probability amplitude.

To study the influence of the initial system-environment correlation on the dynamics of the atomic impurity qubit, we calculate the population amplitude $|\mathcal{K}(t)|$ on the upper state as a function of time t. The numerical results are shown in Fig. 7(a). Then we can obtain from the condition (32) that the bound state is formed when $B_x < 16.8$ Hz. We can see that, when the bound state is absent, i.e., $B_x < 16.8$ Hz, the system decays fast. However, when the bound state is formed, i.e., $B_x < 16.8$ Hz, we find the system dynamics remains unchanged with time t, which confirms our expectation based on the bound-state analysis. In addition, from Fig. 7(a), we can see that there exists a maximum Y (close to 1 but smaller than 1) for $|\mathcal{K}(t)|$ at $t = 0.1$ s where the impurity atom arrives at the maximal population on its excited state. This comes from the feedback of the dipolar Bose-Einstein condensate reservoir on the impurity atom with decoherence suppressed [originated from the second term of Eq. (45)].

However, *in the rectangular wave case*, $\mathcal{M}_k(0)$ that takes the following form:

$$\mathcal{M}_k(0) = \begin{cases} i\eta/\sqrt{S}, & 0 \leqslant k \leqslant T_0, \\ 0, & k > T_0 \end{cases} \tag{47}$$

is shown in Fig. 7(b). The initial system-environment correlation does not alter the non-Markovianity of the impurity atom. But it suppress the population of the impurity atom on its excited state. This environment-induced reactance describes the energy exchange between the system and the environment,

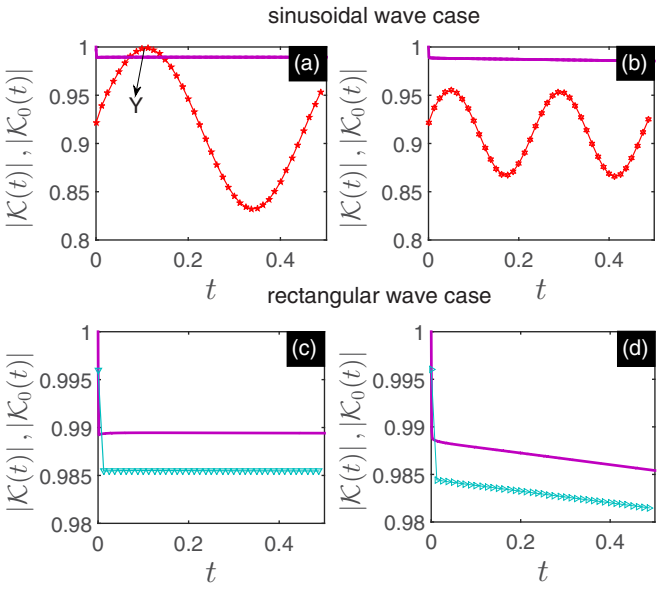

FIG. 7. Influence of the initial system-environment correlation on the dynamics of the AIQ with $\chi = 0$. The solid lines and the pointed lines correspond to the excited-state populations $|\mathcal{K}_0(t)|$ and $|\mathcal{K}(t)|$ with uncorrelated and correlated initial states, respectively. The sinusoidal wave case (46) and rectangular wave case (47) correspond to (a) and (b) [$a = 0.04,\ \Delta_0 = 90,\ \eta = 0.11,\ k_0 = 100,\ T_0 = 2\pi$], (c) and (d) [$\eta = 0.1,\ T_0 = 5$], respectively. The other parameters take $B_x = 10$ Hz for (a) and (c) and $B_x = 100$ Hz for (b) and (d).

reminiscent of the effect of the initial system-environment correlation.

V. DISCUSSIONS WITHOUT THE ROTATING-WAVE APPROXIMATION

In many physical systems described by the Hamiltonian of Eq. (9), the typical coupling strength many orders of magnitude smaller than the frequencies, characterizing the weak-coupling regime. It is then a good approximation to drop the counter-rotating terms, a procedure which is known as the rotating-wave approximation. In this section, we will study the influence of the counterrotating terms on the system dynamics in the AIQ-dBEC model. This can be demonstrated by deriving an effective Hamiltonian in weak-coupling limits by using the Fröhlich-Nakajima transformation.

In order to study the influence of the counterrotating terms in the Hamiltonian, we write Eq. (9) as (here we set $\hbar = 1$)

$$\begin{aligned}\hat{H} &= \hat{H}_0 + \hat{H}_I,\\ \hat{H}_0 &= B_x\hat{\sigma}_z + \sum_k \omega_k \hat{a}_k^\dagger \hat{a}_k,\\ \hat{H}_I &= -\sum_k [g_k(\hat{a}_k + \hat{a}_k^\dagger)\hat{\sigma}_+ + \text{H.c.}].\end{aligned} \tag{48}$$

In order to take into account the correlation between the AIQ and the dBEC, we present a treatment based on a generalized version of the Fröhlich-Nakajima transformation $\exp(\hat{S}_1)$ [69–72].

We can derive the second-order effective Hamiltonian without rotating wave approximation by this unitary transformation:

$$\hat{H}_{\text{eff}} = \exp(\hat{S}_1)\hat{H}\ \exp(-\hat{S}_1) = \hat{H}_0 + \hat{H}_1 + \hat{H}_2 \cdots, \tag{49}$$

where

$$\hat{S}_1 = \sum_k (\xi_k^* \hat{a}_k^\dagger \hat{\sigma}_+ - \xi_k \hat{a}_k \hat{\sigma}_-), \tag{50}$$

with undetermined coefficients ξ_k. A k-dependent function ξ_k is introduced in the transformation, which corresponds to displacements of each boson mode due to the coupling to the two-state system [73–76]. In order to eliminate the counter-rotating terms $\hat{a}_k^\dagger\hat{\sigma}_+ + \text{H.c.}$ from the first-order term, we need impose

$$\begin{aligned}\hat{H}_1 &= \hat{H}_I + [\hat{S}_1, \hat{H}_0]\\ &= \sum_k [-g_k(\hat{a}_k^\dagger + \hat{a}_k)\hat{\sigma}_+ - (2B_x + \omega_k)\xi_k^* \hat{a}_k^\dagger \hat{\sigma}_+ + \text{H.c.}]\\ &= \sum_k -(g_k \hat{a}_k \hat{\sigma}_+ + g_k \hat{a}_k^\dagger \hat{\sigma}_-),\end{aligned} \tag{51}$$

which leads to the coefficient $\xi_k = -g_k/(2B_x + \omega_k)$ and then yields the anti-Hermitian operator $\hat{S}_1$ in Eq. (50). If we omit the high-frequency intercrossing terms such as $\hat{a}_k^\dagger \hat{a}_{k'}^\dagger$, and $\hat{a}_k \hat{a}_{k'}$, we get

$$\begin{aligned}\hat{H}_2 &= [\hat{S}_1, \hat{H}_I] + \frac{1}{2}[\hat{S}_1, [\hat{S}_1, \hat{H}_0]]\\ &= \sum_k \frac{|g_k|^2}{2B_x + \omega_k}\hat{\sigma}_+\hat{\sigma}_- - \sum_k \frac{|g_k|^2}{2B_x + \omega_k}.\end{aligned} \tag{52}$$

Finally, we obtain the effective Hamiltonian $\hat{H}_{\text{eff}} = \exp(\hat{S}_1)\hat{H}\exp(-\hat{S}_1)$ up to the second order in the system-environment coupling constant as follows

$$\hat{H}_{\text{eff}} = \tilde{B}_x\hat{\sigma}_z + \sum_k \omega_k \hat{a}_k^\dagger \hat{a}_k - \sum_k g_k(\hat{a}_k\hat{\sigma}_+ + \hat{a}_k^\dagger\hat{\sigma}_-). \tag{53}$$

Here the modified level spacing for the AIQ that can be regarded as the Lamb shift is

$$\tilde{B}_x = B_x + \frac{1}{2}\sum_k \frac{|g_k|^2}{\omega_k + 2B_x}. \tag{54}$$

We show that the effective Hamiltonian (54) has the same form with the Hamiltonian under the RWA in Hamiltonian (10) except the modified factor B_x. With this observation, we can obtain exact non-Markovian master equation (20) in the initial correlation between the qubit and the dBEC with effective decay given by Eq. (21) by only replacing B_x with $\tilde{B}_x$. With the parameters we have used above, we estimate the maximum value of the coupling strength g_k as 10^{-1} Hz, while $B_x \sim 10$ Hz–100 Hz, so that $g_k \ll B_x$. Therefore, within the parameters we selected (i.e., weak-coupling regime), $\tilde{B}_x \approx B_x$, we do not consider the influence of the counterrotating terms on the atomic impurity qubit Secs. II–IV in this work.

VI. DISCUSSION AND CONCLUSION

To summarize, we have studied the dissipative dynamics of an atomic impurity qubit immersed in the structured environment—a quasi-2D dipolar Bose-Einstein condensate. We discover that the DDI can significantly modify the non-Markovianity. We derive a non-Markovian master equation for the atomic impurity qubit with an initial correlation between AIQ and dBEC, which contains all the influences of the non-Markovian environment on the system. We give an analytical expression for the spectrum density of the coupled AIQ-dBEC system. The result suggests that the DDI-induced excitation spectrum is highly tunable via either the Feshbach resonance or a fast rotating magnetic field. It is remarkable to find that the AIQ may not decay completely to its ground state and population on its excited state could be nonzero in the steady state. This is qualitatively different from the conventional results, and it reveals that the non-Markovian effect may not only cause a quantitative correction to the short-time dynamics, but also induces a qualitative change to the steady state of the quantum system. Further examination shows that such a qualitative change is essentially due to the formation of the system-environment bound state.

This paper focuses on a reservoir and uses it to study quantum non-Markovian dynamics where the environmental spectrum can be well engineered and modulated from being relatively flat to very sharp by the scattering lengths. We found that the DDI strength can increase the sharpness of the environmental spectrum and lead to non-Markovian enhancement. This is different from most studies in the literature where the spectrum of the environment only leads to the loss of coherence.

ACKNOWLEDGMENTS

This work was supported by the National Natural Science Foundation of China (NSFC) under Grants No. 11434011, No. 11421063, No. 11534002, No. 61475033, No. 11775048, and No. 11705025 and Science Foundation of the Education Department of Jilin Province during the 13th Five-Year Plan Period (No. JJKH20190262KJ).

APPENDIX: THE DERIVATION OF NON-MARKOVIAN MASTER EQUATION (20) WITH THE INITIAL CORRELATION

With the help of the probability amplitudes α, $\mathcal{K}(t)$, and $\mathcal{M}_k(t)$ we can now express the reduced density matrix $\rho(t)$ as

$$\rho(t) = \mathrm{Tr}_R|\psi(t)\rangle\langle\psi(t)| \equiv \begin{pmatrix} |\mathcal{K}(t)|^2 & \alpha^*\mathcal{K}(t) \\ \alpha\mathcal{K}^*(t) & 1-|\mathcal{K}(t)|^2 \end{pmatrix}, \quad \text{(A1)}$$

where $|\psi(t)\rangle$ is given by (12) and $\mathrm{Tr}_R\bullet = \langle 0|\bullet|0\rangle + \sum_k \langle 1_k|\bullet|1_k\rangle$. Differentiating Eq. (A1) with respect to time with zero-exciton probability amplitude $\dot{\alpha} = 0$, we get

$$\dot{\rho}(t) = \begin{pmatrix} \dot{\mathcal{K}}(t)\mathcal{K}^*(t) + \text{c.c.} & \alpha^*\dot{\mathcal{K}}(t) \\ \alpha\dot{\mathcal{K}}^*(t) & -\dot{\mathcal{K}}(t)\mathcal{K}^*(t) - \text{c.c.} \end{pmatrix}. \quad \text{(A2)}$$

We assume that the non-Markovian master equation (A2) has the form of Eq. (20), which can be rewritten as

$$\dot{\rho}(t) = \begin{pmatrix} -2\gamma(t)|\mathcal{K}(t)|^2 & -\alpha^*[\gamma(t)+ir(t)]\mathcal{K}(t) \\ -\alpha[\gamma(t)-ir(t)]\mathcal{K}^*(t) & 2\gamma(t)|\mathcal{K}(t)|^2 \end{pmatrix}. \quad \text{(A3)}$$

Comparing Eqs. (A2) and (A3), we can obtain Eq. (22).

[1] H. P. Breuer and F. Petruccione, *The Theory of Open Quantum Systems* (Oxford University Press, Oxford, 2007).

[2] U. Weiss, *Quantum Dissipative Systems* (World Scientific, Singapore, 1999).

[3] F. Caruso, A. W. Chin, A. Datta, S. F. Huelga, and M. B. Plenio, Entanglement and entangling power of the dynamics in light-harvesting complexes, Phys. Rev. A **81**, 062346 (2010).

[4] A. Olaya-Castro, C. F. Lee, F. F. Olsen, and N. F. Johnson, Efficiency of energy transfer in a light-harvesting system under quantum coherence, Phys. Rev. B **78**, 085115 (2008).

[5] S. L. Su, Y. Z. Tian, H. Z. Shen, H. P. Zang, E. J. Liang, and S. Zhang, Applications of the modified Rydberg antiblockade regime with simultaneous driving, Phys. Rev. A **96**, 042335 (2017); S. L. Su, Y. Gao, E. J. Liang, and S. Zhang, Fast Rydberg antiblockade regime and its applications in quantum logic gates, *ibid.* **95**, 022319 (2017); S. L. Su, E. J. Liang, S. Zhang, J. J. Wen, L. L. Sun, Z. Jin, and A. D. Zhu, One-step implementation of the Rydberg-Rydberg-interaction gate, *ibid.* **93**, 012306 (2016).

[6] P. Rebentrost and A. Aspuru-Guzik, Communication: Exciton-phonon information flow in the energy transfer process of photosynthetic complexes, J. Chem. Phys. **134**, 101103 (2011).

[7] M. M. Wolf, J. Eisert, T. S. Cubitt, and J. I. Cirac, Assessing Non-Markovian Quantum Dynamics, Phys. Rev. Lett. **101**, 150402 (2008).

[8] Á. Rivas, S. F. Huelga, and M. B. Plenio, Entanglement and Non-Markovianity of Quantum Evolutions, Phys. Rev. Lett. **105**, 050403 (2010).

[9] H. P. Breuer, E. M. Laine, and J. Piilo, Measure for the Degree of Non-Markovian Behavior of Quantum Processes in Open Systems, Phys. Rev. Lett. **103**, 210401 (2009).

[10] X. M. Lu, X. Wang, and C. P. Sun, Quantum Fisher information flow and non-Markovian processes of open systems, Phys. Rev. A **82**, 042103 (2010).

[11] T. J. G. Apollaro, C. Di Franco, F. Plastina, and M. Paternostro, Memory-keeping effects and forgetfulness in the dynamics of a qubit coupled to a spin chain, Phys. Rev. A **83**, 032103 (2011).

[12] P. Haikka, S. McEndoo, G. De Chiara, G. M. Palma, and S. Maniscalco, Quantifying, characterizing, and controlling information flow in ultracold atomic gases, Phys. Rev. A **84**, 031602(R) (2011).

[13] P. Haikka, J. Goold, S. McEndoo, F. Plastina, and S. Maniscalco, Non-Markovianity, Loschmidt echo, and criticality: A unified picture, Phys. Rev. A **85**, 060101(R) (2012).

[14] B. H. Liu, L. Li, Y. F. Huang, C. F. Li, G. C. Guo, E. M. Laine, H. P. Breuer, and J. Piilo, Experimental control of the transition from Markovian to non-Markovian dynamics of open quantum systems, Nat. Phys. **7**, 931 (2011).

[15] A. Smirne, D. Brivio, S. Cialdi, B. Vacchini, and M. G. A. Paris, Experimental investigation of initial system-environment correlations via trace-distance evolution, Phys. Rev. A **84**, 032112 (2011).

[16] J. S. Tang, C. F. Li, Y. L. Li, X. B. Zou, G. C. Guo, H. P. Breuer, E. M. Laine, and J. Piilo, Measuring non-Markovianity of processes with controllable system-environment interaction, Europhys. Lett. **97**, 10002 (2012).

[17] I. de Vega and D. Alonso, Dynamics of non-Markovian open quantum systems, Rev. Mod. Phys. **89**, 015001 (2017).

[18] P. Haikka, S. McEndoo, G. De Chiara, G. M. Palma, and S. Maniscalco, Robust non-Markovianity in ultracold gases, Phys. Scr., T **151**, 014060 (2012).

[19] P. Haikka, S. McEndoo, and S. Maniscalco, Non-Markovian probes in ultracold gases, Phys. Rev. A **87**, 012127 (2013).

[20] Q. Beaufils, R. Chicireanu, T. Zanon, B. Laburthe-Tolra, E. Marechal, L. Vernac, J. C. Keller, and O. Gorceix, All-optical production of chromium Bose-Einstein condensates, Phys. Rev. A **77**, 061601 (2008).

[21] A. Griesmaier, J. Werner, S. Hensler, J. Stuhler, and T. Pfau, Bose-Einstein Condensation of Chromium, Phys. Rev. Lett. **94**, 160401 (2005).

[22] M. W. Lu, N. Q. Burdick, S. H. Youn, and B. L. Lev, Strongly Dipolar Bose-Einstein Condensate of Dysprosium, Phys. Rev. Lett. **107**, 190401 (2011).

[23] M. W. Lu, N. Q. Burdick, and B. L. Lev, Quantum Degenerate Dipolar Fermi Gas, Phys. Rev. Lett. **108**, 215301 (2012).

[24] K. Aikawa, A. Frisch, M. Mark, S. Baier, A. Rietzler, R. Grimm, and F. Ferlaino, Bose-Einstein Condensation of Erbium, Phys. Rev. Lett. **108**, 210401 (2012).

[25] K. K. Ni, S. Ospelkaus, M. H. G. de Miranda, A. Péer, B. Neyenhuis, J. J. Zirbel, S. Kotochigova, P. S. Julienne, D. S. Jin, and J. Ye, A high phase-space-density gas of polar molecules, Science **322**, 231 (2008).

[26] M. H. G. de Miranda, A. Chotia, B. Neyenhuis, D. Wang, G. Quéméner, S. Ospelkaus, J. L. Bohn, J. Ye, and D. S. Jin, Controlling the quantum stereodynamics of ultracold bimolecular reactions, Nat. Phys. **7**, 502 (2011).

[27] A. Chotia, B. Neyenhuis, S. A. Moses, B. Yan, J. P. Covey, M. Foss-Feig, A. M. Rey, D. S. Jin, and J. Ye, Long-Lived Dipolar Molecules and Feshbach Molecules in a 3D Optical Lattice, Phys. Rev. Lett. **108**, 080405 (2012).

[28] T. Lahaye, C. Menotti, L. Santos, M. Lewenstein, and T. Pfau, The physics of dipolar bosonic quantum gases, Rep. Prog. Phys. **72**, 126401 (2009).

[29] L. Santos, G. V. Shlyapnikov, and M. Lewenstein, Roton-Maxon Spectrum and Stability of Trapped Dipolar Bose-Einstein Condensates, Phys. Rev. Lett. **90**, 250403 (2003).

[30] D. H. J. O'Dell, S. Giovanazzi, and G. Kurizki, Rotons in Gaseous Bose-Einstein Condensates Irradiated by a Laser, Phys. Rev. Lett. **90**, 110402 (2003).

[31] U. R. Fischer, Stability of quasi-two-dimensional Bose-Einstein condensates with dominant dipole-dipole interactions, Phys. Rev. A **73**, 031602(R) (2006).

[32] R. M. Wilson, S. Ronen, J. L. Bohn, and H. Pu, Manifestations of the Roton Mode in Dipolar Bose-Einstein Condensates, Phys. Rev. Lett. **100**, 245302 (2008).

[33] A. Widera, O. Mandel, M. Greiner, S. Kreim, Entanglement Interferometry for Precision Measurement of Atomic Scattering Properties, Phys. Rev. Lett. **92**, 160406 (2004).

[34] R. Mottl, F. Brennecke, K. Baumann, R. Landig, T. Donner, T. Esslinger, Roton-type mode softening in a quantum gas with cavity-mediated long-range interactions, Science **336**, 1570 (2012).

[35] S. C. Ji, L. Zhang, X. T. Xu, Z. Wu, Y. J. Deng, S. Chen, and J. W. Pan, Softening of Roton and Phonon Modes in a Bose-Einstein Condensate with Spin-Orbit Coupling, Phys. Rev. Lett. **114**, 105301 (2015).

[36] M. A. Cirone, G. De Chiara, G. M. Palma, and A. Recati, Collective decoherence of cold atoms coupled to a Bose-Einstein condensate, New J. Phys. **11**, 103055 (2009).

[37] J. B. Yuan, H. J. Xing, L. M. Kuang, and S. Yi, Quantum non-Markovian reservoirs of atomic condensates engineered via dipolar interactions, Phys. Rev. A **95**, 033610 (2017).

[38] B. Vacchini and H. P. Breuer, Exact master equations for the non-Markovian decay of a qubit, Phys. Rev. A **81**, 042103 (2010).

[39] H. P. Breuer, B. Kappler, and F. Petruccione, Stochastic wave-function method for non-Markovian quantum master equations, Phys. Rev. A **59**, 1633 (1999).

[40] H. P. Breuer, E. M. Laine, J. Piilo, and B. Vacchini, *Colloquium*: Non-Markovian dynamics in open quantum systems, Rev. Mod. Phys. **88**, 021002 (2016).

[41] C. Chin, R. Grimm, P. Julienne, and E. Tiesinga, Feshbach resonances in ultracold gases, Rev. Mod. Phys. **82**, 1225 (2010).

[42] H. T. Ng and S. Bose, Single-atom-aided probe of the decoherence of a Bose-Einstein condensate, Phys. Rev. A **78**, 023610 (2008).

[43] H. J. Xing, A. B. Wang, Q. S. Tan, W. X. Zhang, and S. Yi, Heisenberg-scaled magnetometer with dipolar spin-1 condensates, Phys. Rev. A **93**, 043615 (2016).

[44] A. Cabello, Quantum correlations are not contained in the initial state, Phys. Rev. A **60**, 877 (1999).

[45] S. Haroche, M. Brune, and J. M. Raimond, Schrödinger cat states and decoherence studies in cavity QED, Eur. Phys. J.: Spec. Top. **159**, 19 (2008).

[46] G. Amato, H. P. Breuer, and B. Vacchini, Generalized trace distance approach to quantum non-Markovianity and detection of initial correlations, Phys. Rev. A **98**, 012120 (2018).

[47] I. Sargolzahi and S. Y. Mirafzali, Entanglement increase from local interaction in the absence of initial quantum correlation in the environment and between the system and the environment, Phys. Rev. A **97**, 022331 (2018).

[48] J. Dajka, J. Łuczka, and P. Hänggi, Distance between quantum states in the presence of initial qubit-environment correlations: A comparative study, Phys. Rev. A **84**, 032120 (2011).

[49] S. Wißmann 1, B. Leggio, and H. P. Breuer, Detecting initial system-environment correlations: Performance of various distance measures for quantum states, Phys. Rev. A **88**, 022108 (2013).

[50] J. Dajka and J. Łuczka, Distance growth of quantum states due to initial system-environment correlations, Phys. Rev. A **82**, 012341 (2010).

[51] E. Chitambar, A. Abu-Nada, R. Ceballos, and M. Byrd, Restrictions on initial system-environment correlations based on the dynamics of an open quantum system, Phys. Rev. A **92**, 052110 (2015).

[52] S. Lorenzo, F. Plastina, and M. Paternostro, Role of environmental correlations in the non-Markovian dynamics of a spin system, Phys. Rev. A **84**, 032124 (2011).

[53] C. F. Li, J. S. Tang, Y. L. Li, and G. C. Guo, Experimentally witnessing the initial correlation between an open quantum system and its environment, Phys. Rev. A **83**, 064102 (2011).

[54] M. Ringbauer, C. J. Wood, K. Modi, A. Gilchrist, A. G. White, and A. Fedrizzi, Characterizing Quantum Dynamics with Initial System-Environment Correlations, Phys. Rev. Lett. **114**, 090402 (2015).

[55] K. Modi, Operational approach to open dynamics and quantifying initial correlations, Sci. Rep. **2**, 581 (2012).

[56] A. G. Kofman, G. Kurizki, and B. Sherman, Spontaneous and induced atomic decay in photonic band structures, J. Mod. Opt. **41**, 353 (1994).

[57] T. Shi, Y. H. Wu, A. González-Tudela, and J. I. Cirac, Bound States in Boson Impurity Models, Phys. Rev. X **6**, 021027 (2016).

[58] P. Zhang, B. You, and L. X. Cen, Long-lived quantum coherence of two-level spontaneous emission models within structured environments, Opt. Lett. **38**, 3650 (2013).

[59] Q. J. Tong, J. H. An, H. G. Luo, and C. H. Oh, Mechanism of entanglement preservation, Phys. Rev. A **81**, 052330 (2010).

[60] H. Z. Shen, X. Q. Shao, G. C. Wang, X. L. Zhao, and X. X. Yi, Quantum phase transition in a coupled two-level system embedded in anisotropic three-dimensional photonic crystals, Phys. Rev. E **93**, 012107 (2016); H. Z. Shen, H. Li, Y. F. Peng, and X. X. Yi, Mechanism for Hall conductance of two-band systems against decoherence, *ibid.* **95**, 042129 (2017); H. T. Cui, H. Z. Shen, S. C. Hou, and X. X. Yi, Bound state and localization of excitation in many-body open systems, Phys. Rev. A **97**, 042129 (2018); H. Z. Shen, C. Shang, Y. H. Zhou, and X. X. Yi, Unconventional single-photon blockade in non-Markovian systems, *ibid.* **98**, 023856 (2018); H. Z. Shen, S. L. Su, Y. H. Zhou, and X. X. Yi, Non-Markovian quantum Brownian motion in one dimension in electric fields, *ibid.* **97**, 042121 (2018); H. Z. Shen, D. X. Li, S. L. Su, Y. H. Zhou, and X. X. Yi, Exact non-Markovian dynamics of qubits coupled to two interacting environments, *ibid.* **96**, 033805 (2017).

[61] Y. Liu and A. A. Houck, Quantum electrodynamics near a photonic bandgap, Nat. Phys. **13**, 48 (2017).

[62] L. Krinner, M. Stewart, A. Pazmiño, J. Kwon, and D. Schneble, Spontaneous Emission in a Matter-Wave Open Quantum System, Nature (London) **559**, 589 (2018).

[63] S. Noda, M. Fujita, and T. Asano, Spontaneous-emission control by photonic crystals and nanocavities, Nat. Photonics **1**, 449 (2007).

[64] P. Lodahl, A. F. Van Driel, I. N. Nikolaev, A. Irman, K. Overgaag, D. Vanmaekelbergh, and W. L. Vos, Controlling the dynamics of spontaneous emission from quantum dots by photonic crystals, Nature (London) **430**, 654 (2004).

[65] S. Bochner and K. Chandrasekharan, *Fourier Transforms* (Princeton University Press, Princeton, 1949).

[66] H. B. Liu, J. H. An, C. Chen, Q. J. Tong, H. G. Luo, and C. H. Oh, Anomalous decoherence in a dissipative two-level system, Phys. Rev. A **87**, 052139 (2013); Q. J. Tong, J. H. An, H. G. Luo, and C. H. Oh, Quantum phase transition in the delocalized regime of the spin-boson model, Phys. Rev. B **84**, 174301 (2011).

[67] W. M. Zhang, P. Y. Lo, H. N. Xiong, M. W. Y. Tu, and F. Nori, General Non-Markovian Dynamics of Open Quantum Systems, Phys. Rev. Lett. **109**, 170402 (2012).

[68] S. Wißmann, A. Karlsson, E. M. Laine, J. Piilo, and H. P. Breuer, Phys. Rev. A **86**, 062108 (2012).

[69] H. Fröhlich, Theory of the superconducting state. I. The ground state at the absolute zero of temperature, Phys. Rev. **79**, 845 (1950).

[70] H. Fröhlich, Interaction of electrons with lattice vibrations, Proc. R. Soc. London, Ser. A **215**, 291 (1952).

[71] S. Nakajima, Perturbation theory in statistical mechanics, Adv. Phys. **4**, 363 (1955).

[72] Q. Ai, Y. Li, H. Zheng, and C. P. Sun, Quantum anti-Zeno effect without rotating wave approximation, Phys. Rev. A **81**, 042116 (2010).

[73] H. Zheng, Dynamics of a two-level system coupled to Ohmic bath: a perturbation approach, Eur. Phys. J. B **38**, 559 (2004).

[74] Z. Lü and H. Zheng, Quantum dynamics of the dissipative two-state system coupled with a sub-Ohmic bath, Phys. Rev. B **75**, 054302 (2007).

[75] H. Zheng, Variational approach to the quantum lattice fluctuations in the Su-Schrieffer-Heeger model: The ground state, Phys. Rev. B **50**, 6717 (1994).

[76] H. Zheng, Long-range order and phase transition in a cooperative Jahn-Teller system, Phys. Rev. B **61**, 1088 (2000).